

Architecture and finite precision optimization for layered LDPC decoders

Cédric Marchand · Laura Conde-Canencia · Emmanuel Boutillon

Received: date / Accepted: date

Abstract Layered decoding is known to provide efficient and high-throughput implementation of LDPC decoders. However, two main issues affect performance and area of practical implementations: quantization and memory. Quantization can strongly degrade performance and memory area can constitute up to 70% of the total area of the decoder implementation. This is the case of the DVB-S2,-T2 and -C2 decoders when considering long frames. This paper is then dedicated to the optimization of these decoders. We first focus on the reduction of the number of quantization bits and propose solutions based on the efficient saturation of the channel values, the extrinsic messages and the a posteriori probabilities (APP). We reduce from 6 to 5 the number of quantization bits for the channel and the extrinsic messages and from 8 to 6 the APPs, without introducing any performance loss. We then consider the optimization of the size of the extrinsic memory, based on the multiple code rates considered by the decoder. The paper finally presents an optimized fixed-point architecture of a DVB-S2 layered decoder and its implementation on an FPGA device.

Keywords

Low-density parity-check (LDPC) code, layered decoding, VLSI implementation, DVB-S2.

1 Introduction

Low-Density Parity-Check (LDPC) codes were initially proposed by Gallager in the early 60's [1], but they

were not used for three decades. This was mainly because the technology was not mature enough for practical implementation. LDPC codes were rediscovered by MacKay [2] in 1995 and are now included in many standards. The existing standards can be categorized into two type of standards: the standards using short frames (648, 1296 and 1944 bits for Wi-Fi) and the standards using long frames (16200 and 64800 bits for DVB-S2). The use of long frames makes it possible to get closer to the Shannon limit, but leads to delays that are not suitable for internet protocols or mobile phone communications. On the other hand, long frames are suitable for streaming or Digital Video Broadcasting (DVB). The 2nd Generation Satellite Digital Video Broadcast (DVB-S2) standard was ratified in 2005, the 2nd Generation Terrestrial DVB (DVB-T2) standard was adopted in 2009 and the 2nd Generation Cable DVB (DVB-C2) was adopted during 2010. These three DVB standards include a common Forward Error Correction (FEC) block. The FEC is composed of an LDPC inner code and BCH outer code. The FEC supports eleven code rates for the DVB-S2 standard frames and six code rates for the DVB-T2 standard frames. In the following, DVB-X2 stands for DVB-S2, -T2, -C2. The LDPC codes defined by the DVB-X2 standards are structured codes or architecture-aware codes (AA-LDPC) [3] and they can be efficiently implemented using the layered decoder architecture [4–6]. The layered decoder benefits from three architecture improvements: parallelism of structured codes, turbo message passing, and Soft-Output (SO) based Node Processor (NP) [4–6].

Even if the state-of-the-art decoder architecture converges to the layered decoder solution, the search of an efficient trade-off between area, cost, low consumption, high throughput and high performance still make the implementation of the LDPC decoder a challenge. Fur-

C. Marchand · L. Conde-Canencia · E. Boutillon
Université Européenne de Bretagne
Lab-STICC, CNRS, UBS
BP 92116 56321 Lorient, France.
E-mail: firstname.surname@univ-ubs.fr

thermore, the designer has to deal with many possible choices of algorithm, parallelism, quantization parameters, code rates and frame lengths. In this article, we study the optimization of the layered decoders. We consider the DVB-S2 standard for comparison with previous designs in literature. However, our work can also be applied to the Wi-Fi and WiMAX LDPC standards, or more generally, to any layered LDPC decoder.

The well-known Min-Sum algorithm [7] and its variants significantly reduce the memory requirements thanks to the compression of the extrinsic messages. For this reason, we consider the Min-Sum algorithm for our study. We also consider the Sum-Product algorithm for comparison in terms of memory area.

The natural way to reduce the memory needs is to use a minimum number of bits to represent the data in the circuit. This can be done first by an appropriate scaling of the input symbol, second by an appropriate saturation of internal data. One should note that using a minimum number of bits to represent data also leads to a reduction in the complexity of the interconnection routing scheme, the area of the processing units and their associated critical path. In the state-of-the-art, the method that the SO and the extrinsic messages are saturated is rarely explicitly explained. In this article, we will discuss efficient saturation of the channel values, the extrinsic messages and the SO values. We also present some ideas related to the efficient use of saturation which leads to significant memory savings. Finally, we introduce a methodology to optimize the implementation of the extrinsic memory under the constraints of 11 code rates and a single port RAM.

The paper is organized as follows: Section 2 presents the layered decoder and the Min-Sum sub-optimal algorithm. In Section 3, we explain the saturating process. Section 4 deals with the optimization of the size of the extrinsic memory. Finally, simulation and synthesis results are provided in Section 5.

2 LDPC decoder and Layered LDPC decoder

In this Section we first overview the principles of LDPC decoding and then focus on the layered decoding approach and architecture.

2.1 LDPC code decoding principles

An LDPC code is defined by its parity-check matrix \mathbf{H} of M rows by N columns. Each column in \mathbf{H} is associated with one bit of the codeword, and each row corresponds to a parity check equation. A nonzero element in a row means that the corresponding bit contributes to

the parity check equation. The set of valid code words $x \in C$ satisfy the equation:

$$x \cdot \mathbf{H}^t = 0, \forall x \in C \quad (1)$$

An LDPC decoder can be described by a Tanner graph [8] which is a graphical representation of the associations between code bits and parity-check equations. Code bits are represented by Variable Nodes (VN) and parity-check equations are represented by Check Nodes (CN), with edges connecting them accordingly to the parity check matrix. A message going from CN c to VN v is called $M_{c \rightarrow v}$, and a message going from VN v to CN c is called $M_{v \rightarrow c}$.

The decoding iterative process known as the Belief Propagation (BP) algorithm, was first introduced by Gallager [1] and rediscovered by MacKay [9]. This algorithm propagates probability messages to the nodes through the edges. These messages provide soft information about the state (0 or 1) of a VN. The Log-BP algorithm considers the probability messages in the log domain and are called Log Likelihood Ratios (LLR). The LLRs are defined as:

$$LLR_v = \log \left(\frac{P(v=0)}{P(v=1)} \right) \quad (2)$$

where $P(v=x)$ is the probability that bit v equals x .

The order in which the nodes are updated is called the scheduling. The flooding schedule, first proposed by Gallager [1] consists in four steps as follows:

2.1.1 Initialization

Set all the $M_{v \rightarrow c}$ to the channel LLR values, i.e: $\forall(c, v)$ such that $\mathbf{H} = 1$, $M_{v \rightarrow c} = LLR_v$.

2.1.2 CNs update

The update of a node means that a node reads the incoming messages and then updates the outgoing messages. For all the CNs, update of the messages by applying the Bayes law in the logarithmic domain. For implementation convenience, the sign and the absolute value of the $M_{c \rightarrow v}$ messages are updated separately:

$$sign(M_{c \rightarrow v}^{new}) = \prod_{v' \in v_c/v} sign(M_{v' \rightarrow c}) \quad (3)$$

$$|M_{c \rightarrow v}^{new}| = f \left(\sum_{v' \in v_c/v} f(|M_{v' \rightarrow c}|) \right) \quad (4)$$

where v_c is the set of all the VNs connected to CN c and v_c/v is v_c without v . The function $f(x)$ is expressed by the equation:

$$f(x) = -\ln \tanh\left(\frac{x}{2}\right) = \ln \frac{\exp x + 1}{\exp x - 1} \quad (5)$$

2.1.3 VNs update

All the VNs are updated. The VN update is performed in two steps. First, equations the Soft Output (SO) value is computed as in (6) where the LLR_v^{in} value is the initial soft input from the channel. Then, the new $M_{v \rightarrow c}$ messages are computed as in (7).

$$SO_v = LLR_v^{in} + \sum_{c \in c_v} M_{c \rightarrow v} \quad (6)$$

$$M_{v \rightarrow c} = SO_v - M_{c \rightarrow v} \quad (7)$$

2.1.4 Hard decision and stopping criteria

If a codeword is found or a maximum number of iteration is reached then the decoding process stop, else the iterative process continues in step two. At the end of the iterative process, a hard decision is made on the VN to output the codeword. The word estimation \hat{y} is given by the hard decision of the SO: $\hat{y}_v = \text{sign}(SO_v)$, $v \in [0, \dots, N]$ where $\text{sign}(x) = 0$ if $x > 0$ and $\text{sign}(x) = 1$ if $x < 0$. If $\hat{y} \cdot \mathbf{H}^t = 0$ then a codeword has been found.

From an implementation point of view, the flooding scheduling LDPC decoder is not optimized. Major improvements have been proposed in the literature, leading to the horizontal layered decoder which is currently the most efficient LDPC decoder architecture and can be applied to the DVB-X2 matrices.

2.2 Horizontal Layered decoder

The layered decoder constitutes an optimized solution for LDPC decoding in terms of convergence speed, parallelism, latency, memory requirements and complexity. These are based on the following features:

2.2.1 The turbo message passing schedule [10, 3]

The CNs are processed one by one. The VNs connected to an updated CN are immediately updated with newly generated $M_{c \rightarrow v}$ messages. The next CNs will thus benefit from newly updated VNs which improves the convergence speed.

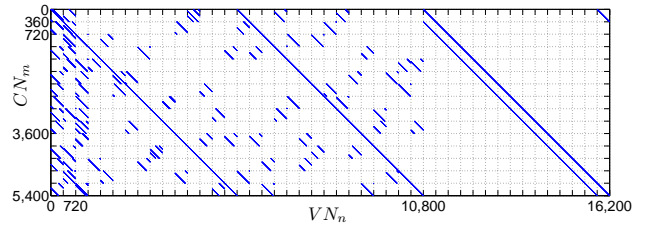


Fig. 1 Block-structured rate-2/3 DVB-S2 matrix (N=16200)

2.2.2 Structured matrices

The Group Horizontal Shuffle or Layered Horizontal Shuffle [5] follows the same scheduling principle as the turbo message passing, but instead of processing the CNs one by one, they are processed by groups. This is possible when the LDPC matrix is composed of identity matrices of size P . Then a group of P CNs can be processed in parallel. The IEEE WiMAX standard [11] uses this matrix structure leading to efficient decoding architectures as the one presented in [4]. Figure 1 shows the structure of the rate-2/3 short-frame DVB-S2 LDPC parity check matrix. This structured matrix is composed of shifted identity matrices of size $P = 360$, allowing for parallel processing of up to 360 CNs.

2.2.3 SO centric decoder

Hereafter we present how the SO-centric NP architecture is deduced. The update of the VNs connected to a given CN is done serially in three steps. First, the message $M_{v \rightarrow c}$ is calculated using (8):

$$M_{v \rightarrow c} = SO_v - M_{c \rightarrow v}^{old} \quad (8)$$

The second step is the serial $M_{c \rightarrow v}$ update as described in equations (3) and (4). Finally, the third step is the calculation of the SO_{new} value:

$$SO_v^{new} = M_{v \rightarrow c} + M_{c \rightarrow v}^{new} \quad (9)$$

Because the $M_{v \rightarrow c}$ is calculated from the SO_v and $M_{c \rightarrow v}^{old}$ values, the SO-centric decoder does not need to save the $M_{v \rightarrow c}^{old}$ values, leading to memory saving.

2.3 Architecture overview

From equations (8) and (9), the NP architecture in Fig. 2 can be derived. The left adder of the architecture performs equation (8) and the right adder performs equation (9). The central part is in charge of the serial $M_{c \rightarrow v}$ update.

Several CNs may be grouped together to form a layer, whenever the column weights in the layer does not

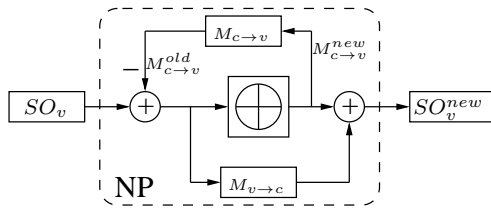


Fig. 2 Check Node centric Node Processor

exceed one. The structured matrices made of identity matrices of size P allow us to compute layers made of P CNs. The layered decoder architecture is mainly based on P NPs that first read serially the Groups of P VNs (VNGs) linked to one Group of CN (CNG). Then after a given number of cycles ϵ , i.e. the NP latency, the P NPs write back the result to the VNGs in the same order.

Pipelining allows a more efficient use of the NP and an increase of the throughput [12–16]. The pipelining consists in reading the v_{c_i} of one sub-iteration while writing on $v_{c_{i-1}}$ the result of the previous sub-iteration. This means that as soon as the reading of one sub-iteration is finished, a new one is started. The corresponding maximum throughput is given by:

$$D = \frac{64800 \cdot F_{clk}}{d_c \cdot \frac{M}{P} \cdot N_{it} + d_c + \epsilon + init} \quad bit.s^{-1} \quad (10)$$

where N_{it} is the number of iterations to decode a codeword, M is the number of CN, P is the number of NPs working in parallel, d_c is the average number of VNs linked to a CN, $init$ is the number of cycle required to init the decoder, F_{clk} is the clock frequency and K is the number of information bits in a codeword.

The central part of Fig. 2 manages the serial $M_{c \rightarrow v}$ update described in equation 4. The $f(x)$ function shown in this equation is difficult to implement. This function can be implemented using look up tables or linear piecewise approximation [17], but can also be implemented more efficiently by using a sub-optimal algorithm as described in the following subsection.

2.4 The normalized Min-Sum algorithm and other related algorithms

The most used sub-optimal algorithms are improved versions of the well-known Min-Sum algorithm [7] such as: the normalized Min-Sum algorithm, the Offset Min-Sum algorithm, the A-min* algorithm [18], the λ -min algorithm [19] and related [20]. The advantages of these algorithms are the simplified computation of equation

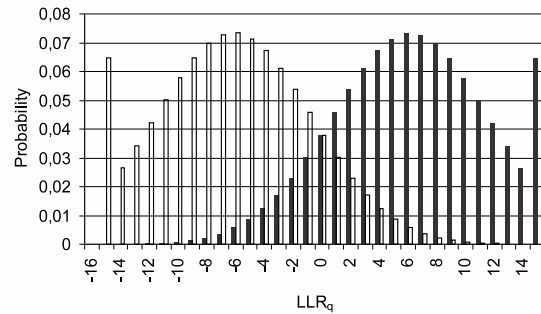


Fig. 3 Resulting distribution of a quantized BPSK modulation

(4) and the compression of the $M_{c \rightarrow v}$ messages. Although all these algorithms present different performances, the memory space they require to store the $M_{c \rightarrow v}$ messages is identical (considering $\lambda = 2$ for the λ -min algorithm). Hence, without loss of generality, for the rest of the paper, we will consider the normalized Min-Sum algorithm. With this algorithm, equation (4) becomes:

$$|M_{c \rightarrow v}^{new}| = \alpha \min_{v' \in v_c/v} |M_{v' \rightarrow c}| \quad (11)$$

where α is the normalization factor, $0 < \alpha \leq 1$.

The CN generates two different values: *Min* and *Submin*. The *Min* value is the normalized minimum of all the incoming $M_{v \rightarrow c}$ values and the *Submin* is the second normalized minimum. Let $Index_{min}$ be the index of the minimum. For each $|M_{c \rightarrow v}^{new}|$ value, if the index of $M_{c \rightarrow v}^{new}$ is $Index_{min}$ then $|M_{c \rightarrow v}^{new}| = submin$, else $|M_{c \rightarrow v}^{new}| = Min$. The $M_{c \rightarrow v}$ from one CN can be compressed into four elements, i.e. *Min*, *Submin*, $Index_{min}$ and $sign(M_{c \rightarrow v}^{new})$. For matrices with a check node degree greater than four, this compression leads to significant memory savings.

3 Saturation

An SO value is the sum of the channel LLR with all the incoming extrinsic messages. Considering the case of the LDPC codes from the DVB-S2 standard, the maximum variable node degree (d_v) is 13. Even if the channel LLR and the $M_{c \rightarrow v}$ are quantized on 6 bits, the SO values must be quantized on 10 bits to prevent overflows. However, to avoid prohibitive word sizes, efficient saturation of the values can significantly reduce the size of the data.

3.1 Channel LLR saturation

For floating point simulation, it is known that the decoders using the Normalized Min-Sum algorithm are not sensitive to scaling in the LLR_{in} values. During the initializing process, the equation $LLR_{in} = 2y/\sigma^2$ can be simplified to $LLR_{in} = y$, saving the need to compute the variance. The received y value is quantized in a way to have integer values at the input of the decoder. We assume here that the quantized value of y denoted by LLR_q is represented on n_{LLR} bits and that the quantification function is defined as:

$$LLR(y)_q = \left[\text{sat}(y, R) \times \frac{2^{n_{LLR}-1} - 1}{R} + 0.5 \right], \quad (12)$$

where $\text{sat}(a, b) = a$ if a belongs to $[-b, b]$ and $\text{sat}(a, b) = \text{sign}(a) \times b$ otherwise. The R value is the interval range of quantization (y is quantized between $[-R, R]$) and also represents the saturation threshold value. Considering the BPSK modulation, we saturate y at $R = 1 + \beta$.

Fig. 3 shows the Probability Density Function of a quantized BPSK modulation (-1 and +1) that is perturbed by an Additive White Gaussian Noise (AWGN) of variance $\sigma = 0.866$ (corresponding to $E_b/N_0 = 2$ dB). The channel is quantized on 5 bits and the saturation threshold is $R = 1 + \beta = 2.47$. The distribution filled in black shows the +1 offset, and the unfilled distribution is the -1 offset. The quantized distribution varies from $LLR_q^{min} = -(2^4 - 1)$ to $LLR_q^{max} = 2^4 - 1$. The problematic is to find the saturation threshold providing the best performance for a given number of bits of quantization. If the saturation threshold is low, then the information given by the tail of the Gaussian curve is saturated. If the threshold is high, then the quantization step increases. The precision is then reduced and the Root Mean Square (RMS) value of the quantization error increases (proportionally with the quantization step).

The saturation limit $1 + \beta$ can be calculated so that the proportion of saturated values is equal to the average proportion of the other values. The average proportion of a given value is $1/(2^{n_{LLR}} - 1)$ (probability of a value in a uniform distribution). On the other side of the equality, the Cumulative Distributive Function (CDF) of a -1 offset distribution applied to the negative saturation limit will give the proportion of saturated values for a -1 offset signal. The equality can be written as:

$$\frac{1}{2} \left[1 + \text{erf} \left(\frac{-\beta}{\sqrt{2}\sigma} \right) \right] = \frac{1}{2^{n_{LLR}} - 1} \quad (13)$$

From equation (13), β can be deduced:

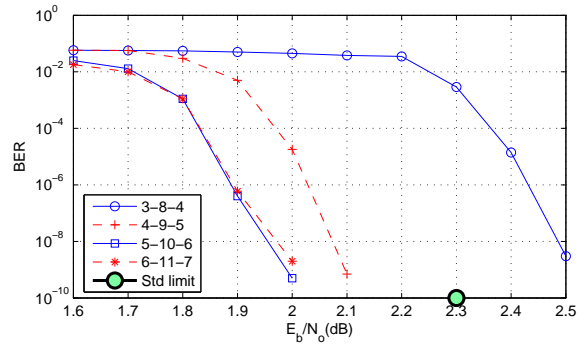


Fig. 4 Effect of the channel LLR quantization on the BER performance. Simulation of a rate-2/3 long frame over the AWGN channel.

$$\beta = \sigma \times \sqrt{2} \left(\text{erf}^{-1} \left(\frac{2^{n_{LLR}} - 1}{2^{n_{LLR}} + 1} \right) \right) \quad (14)$$

Thus the β value is a function of n_{LLR} and proportional to σ . By applying equations (14) and (12), the optimum saturation threshold and the scaling factor can be computed. The problem of this solution is that an adaptive quantization of y is needed that requires a channel estimation of σ .

In fact, to prevent the σ computation, an optimal scaling factor is calculated for a given SNR. If the performance requirement is reached for a given SNR, then for a higher SNR, the quantization would be sub-optimal. However, even with sub-optimal quantization, with a higher SNR, the performance continues to improve. For each code rate, a constant scaling factor ω and saturation value $1 + \beta$ can be pre-computed saving the need for the σ value.

3.1.1 Effects of the channel LLR saturation on BER performance

Fig. 4 shows the simulation results for a normalized Min-Sum fixed-point layered decoder, with a maximum of 30 iterations, long frame, and code rate 2/3 in AWGN channel. The normalization factor is $\alpha = 0.75$. We consider the following notation: a 3-8-4 configuration refers to channel LLRs quantized on 3 bits, an SO value word size of 8 bits and a $M_{c \rightarrow v}$ word size of 4 bits. In Fig. 4 "Std limit" corresponds to the standard limit, which is set at 1 dB from the Shannon limit. The quantization values of the $M_{c \rightarrow v}$ messages and SO values are not optimized and are chosen to be large enough so that they do not affect the results of the channel quantization. Fig. 4 shows that a quantization on 4 or 5 bits of the LLR_{in} is enough to fulfill the standard requirements.

3.2 SO saturation

Once the LLR_{in} are quantized, they are stored in an SO memory that evolves with the iterative process. This SO memory needs to be saturated to limit its size.

3.2.1 The problem of SO saturation

Let us first consider the saturation case where $SO_{max} < SO_v^{new}$ during the SO update (9). The saturation process will bound SO_v^{new} to the SO_{max} value. This will introduce an error ϵ_v in the SO_v^{new} value ($\epsilon = SO_v^{new} - SO_{max}$). During the next iteration, the new $M'_{v \rightarrow c}$ value will be $M'_{v \rightarrow c} = SO_v - M_{c \rightarrow v} = M_{v \rightarrow c} - \epsilon_v$.

Let us also consider the worst case: during an iteration, SO_v is saturated at $+SO_{max}$, each CN confirms a positive $M_{c \rightarrow v}$ value, and $d_v=13$ (i.e. SO_v is saturated 13 times). At the beginning of the next iteration, $SO_v = SO_{max}$. From (8) and (9), we can deduce that $SO_{new} = SO_{old} + \Delta M_{c \rightarrow v}$ where $\Delta M_{c \rightarrow v} = M_{c \rightarrow v}^{new} - M_{c \rightarrow v}^{old}$. If $\Delta M_{c \rightarrow v} < 0$, the SO value decreases. The SO value can even decrease 13 times and change its sign. To summarize, with the SO saturation, the SO value cannot increase, but it can decrease. The saturation introduces a non-linearity that can produce pseudo-codewords and an error floor. In the next section we propose a solution to overcome this problem.

3.2.2 A solution for SO saturation

The solution that we propose was first introduced in [21] and relies partially on the A Prioxy Probability (APP) based decoding algorithm [7]. The APP-variable decoding algorithm simplifies equation (8) to:

$$M_{v \rightarrow c} = SO_v \quad (15)$$

which greatly reduces the architecture complexity but introduces significant performance loss. The idea is to use equation (15) only when there is saturation. This leads to the APP-SO saturation algorithm, which is described as follows:

Algorithm 1 APP-SO saturation algorithm

```

if  $SO_v = SO_{max}$  then
   $M_{v \rightarrow c} = SO_v$ 
else
   $M_{v \rightarrow c} = SO_v - M_{c \rightarrow v}$ 
end if

```

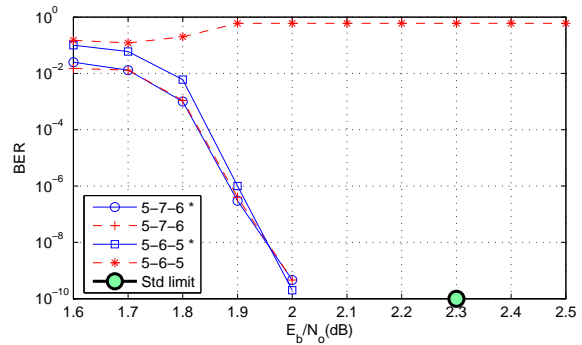


Fig. 5 Effect of the channel LLR quantization on the BER performance. Simulation of a rate-2/3 long frame over the AWGN channel.

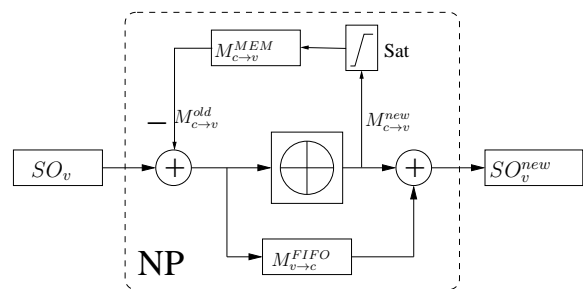


Fig. 6 NP with saturation of the extrinsic messages

3.2.3 Effects of the SO saturation on the BER performance

Fig. 5 shows the simulation results using the same conditions as in Fig. 4. An asterisk symbol in the legend means that the APP-SO algorithm is used. The results show that with the APP-SO algorithm it is possible to reduce the number of SO quantization bits from 7 to 6 without performance loss (compare curves 5-7-6 and 5-6-5*). However, without considering the APP-SO algorithm this one-bit reduction would lead to dramatic performance loss (curve 5-6-5).

3.3 Saturation of the extrinsic messages

Fig. 6 shows the SO based node processor. The newly updated extrinsic $M_{c \rightarrow v}^{new}$ is used to compute SO_v^{new} from equation (9). $M_{c \rightarrow v}^{new}$ is also stored in the extrinsic memory for the calculation of $M_{v \rightarrow c}$ (8) at the next iteration. Any saturation on the value $M_{c \rightarrow v}^{new}$ responsible for the SO update would not produce area savings and would degrade performance. This is the reason why we do not saturate this value. On the other hand, saturation of the $M_{c \rightarrow v}^{new}$ messages that are stored in a memory would lead to significant area savings. Furthermore, the saturation of the $M_{c \rightarrow v}^{new}$ stored in the extrinsic memory is much less critical because it will be used only once

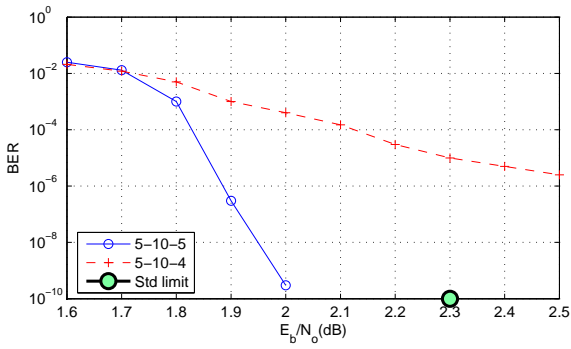


Fig. 7 Effect of the extrinsic message saturation on the BER performance. Simulation of a rate-2/3 long frame over the AWGN channel.

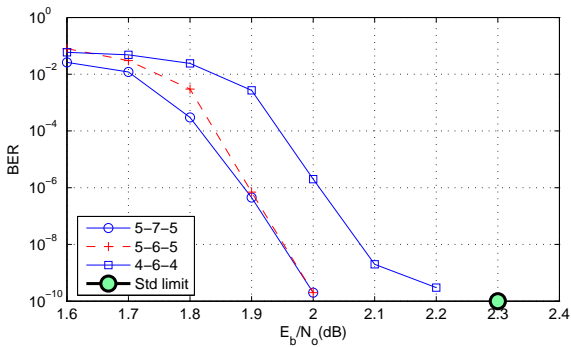


Fig. 8 Effect of the SO and the extrinsic message saturation on the BER performance. Simulation of a rate-2/3 long frame over the AWGN channel.

during an iteration to compute an $M_{v \rightarrow c}$. Furthermore, this computed $M_{v \rightarrow c}$ will affect SO^{new} only if it is a minimum value (see equation (11)).

3.3.1 Effects of the extrinsic message saturation on the BER performance

Fig. 7 shows the simulation results using the same conditions as in Fig. 4. Using the same number of bits for the LLR and the extrinsic messages quantization, i.e., $n_{LLR} = n_{ext} = 5$, results in performance results within the standard requirement. However, considering $n_{ext} < n_{LLR} = 5$, leads to dramatic performance loss.

3.4 Combining the SO and the extrinsic saturation processes

Fig. 8 shows the simulation results when combining the APP-SO saturation algorithm with the extrinsic saturation. These results show that the quantization and saturation solution we propose makes it possible to reduce the 6-8-6 configuration to a 4-6-4 configuration that respects the standard requirements. Considering a

Rate	M	W_{Sign}	W_{Index}	$W_{M_{c \rightarrow v}}$	Memory
1/4	48600	4	2	14	680400
1/3	43200	5	3	16	691200
2/5	38880	6	3	17	660960
1/2	32400	7	3	18	583200
3/5	25920	9	3	21	544320
2/3	21600	10	4	22	475200
3/4	16200	14	4	26	421200
4/5	12960	18	5	31	401760
5/6	10800	22	5	35	378000
8/9	7200	27	5	40	288000
9/10	6480	30	5	43	278640

Table 1 Memory size of extrinsic messages as a function of the DVB-S2 code rates when implementing the Min-Sum algorithm

5-6-5 configuration leads to performance gains of about 0.1 or 0.2 dB, compared to the 4-6-4 configuration.

3.5 Conclusion on the saturation optimization

The analysis of the saturation process shows that a better trade-off between word size and performance can be obtained with an efficient saturation of the LLR_{in} , the SO and the extrinsic values. Simulations show the robustness of our saturation solutions allowing for the use of fewer bits than the usual 6-8-6 configuration. To be specific, the 5-6-5 configuration leads to quantization bit saving while providing the same performance as any other known implementation.

4 Optimizing the size of the extrinsic memory

The decoder requirements in terms of extrinsic memory size strongly depend on the coding rate. In this section we focus on the design of an optimal decoder implementation that supports all the DVB-S2 standard code rates.

4.1 Memory size

The memory requirements of each CN is determined by the $M_{c \rightarrow v}^{old}$ messages needed for the CN computation. In the case of the normalized Min-Sum algorithm [7], the $M_{c \rightarrow v}^{old}$ values are compressed with Min , $Submin$, $index_{min}$ and $Sign(M_{c \rightarrow v})$. In terms of memory, one address must be allocated for every CN, which means that the RAM address range (R_{RAM}) is given by the number of CNs (M). The RAM word size (W_{RAM}) is given by the size of the compressed $M_{c \rightarrow v}^{old}$ values. If we denote by W_h the word size of h , then $W_{M_{c \rightarrow v}} = W_{|Min|} + W_{|Submin|} + W_{Index} + W_{Sign}$. Table 1 presents

the required memory capacity ($M \times W_{M_{c \rightarrow v}}$) for each rate. To calculate $W_{M_{c \rightarrow v}}$, we give $W_{|Min|}$ and $W_{|Submin|}$ a constant value of 4. To handle the eleven code rates of the standard, a simple implementation would define R_{RAM} with the maximum M value, and W_{RAM} with the maximum $W_{M_{c \rightarrow v}}$ in Table 1. The total memory capacity would give: $48600 \times 43 = 2089800$ bits. For rate 1/4, 67% of word bits are wasted but addresses are fully used. On the other hand, for rate 9/10, word bits are fully used but 86 % of the addresses are wasted. Theoretically, a memory size of 691200 bits would be enough to cover all the rates. A solution needs to be found for a better utilization of the memory.

4.2 Optimization principle

The idea is to add flexibility to both the address range and the word size. For this, we benefit from the fact that the RAM that stores the compressed $M_{c \rightarrow v}^{old}$ value is needed only once per layer. The delay to compute the next layer is of d_c cycles, so we can use up to d_c cycles to fetch the data in the memory. A word can be split into two if we take two cycles to fetch the data, and split in three if we take three cycles. If we consider a single port RAM to implement the memory, up to $\lfloor d_c/2 \rfloor$ cycles can be used to read data, and $\lfloor d_c/2 \rfloor$ cycles to write new data.

Let us consider the example of a memory bank of size $48600(R_{RAM}) \times 22(W_{RAM})$. In a first configuration, where one cycle is used, we have a memory size of 48600×22 . This first configuration fits the rates 1/4, 1/3, 2/5, 1/2, 3/5, and 2/3. In a second configuration, where two cycles are used and two words of size 22 are fetched at consecutive addresses, we have the equivalent of a memory of size 24300×44 which fits the rates 3/4, 4/5, 5/6, 8/9 and 9/10. The total memory size for the two-cycle option is equal to $48600 \times 22 = 1069200$ bits. This constitutes a memory saving of 50% compared to the straightforward implementation.

4.3 Results

The previously described process can be used for different word sizes. Table 2 gives an example with $W_{RAM} = 9$. For each rate, the number of cycles is given by:

$$n_{cycles} = \lceil W_{M_{c \rightarrow v}} / W_{RAM} \rceil$$

The RAM range for a code rate R_{RAM} is deduced from $R_{RAM} = n_{cycles} \times M$. The global RAM range (R_{RAM}^{global}) is given by the maximum R_{RAM} in Table 2 and the total memory capacity is $R_{RAM}^{global} \times W_{RAM} = 97200 \times 9 = 874800$ bits.

Rate	M	$W_{M_{c \rightarrow v}}$	n_{cycles}	R_{RAM}
1/4	48600	14	2	97200
1/3	43200	16	2	86400
2/5	38880	17	2	77760
1/2	32400	18	2	64800
3/5	25920	21	3	77760
2/3	21600	22	3	64800
3/4	16200	26	3	48600
4/5	12960	31	4	51840
5/6	10800	35	4	43220
8/9	7200	40	5	36000
9/10	6480	43	5	32400

Table 2 Memory capacity of the extrinsic message with $W_{RAM} = 9$

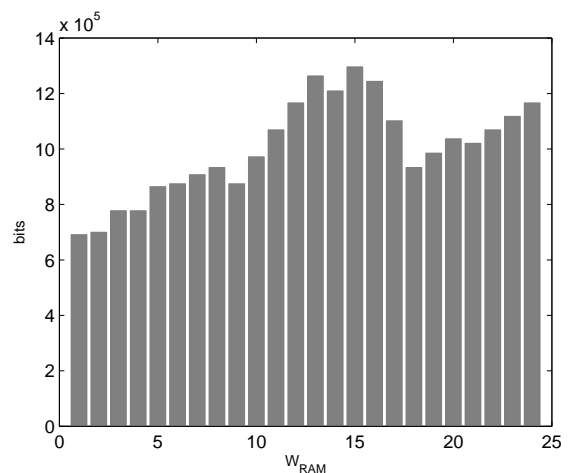


Fig. 9 Memory capacity as a function of W_{RAM}

Fig. 9 shows the total memory capacity as a function of the word length W_{RAM} . There are local minima for word sizes 1, 9, 14, 18 and 21 bits. As the number of clock cycle to fetch $M_{c \rightarrow v}^{old}$ is bounded by $\lfloor d_c/2 \rfloor$, the possible solutions are limited to W_{RAM} values greater than 7. A word size of 9 bits gives the best memory optimization of 874800 bits. This is only 26 % more than the theoretical minimum memory size.

4.4 Case of the Sum-Product algorithm

When using a Sum-Product algorithm [22–24] instead of a Min-Sum algorithm, the CN update equation (4) is computed for each $M_{c \rightarrow v}$ value and then each $M_{c \rightarrow v}$ value is stored. The process described in subsection 4.2 can be used, but a simpler and more efficient implementation is also possible. We consider the architecture overview of Fig. 2 with a dual port RAM that stores the $M_{c \rightarrow v}$ values. At every cycle, a $M_{c \rightarrow v}^{new}$ value is stored and a $M_{c \rightarrow v}^{old}$ value is read from the dual port RAM simultaneously. The address range of this mem-

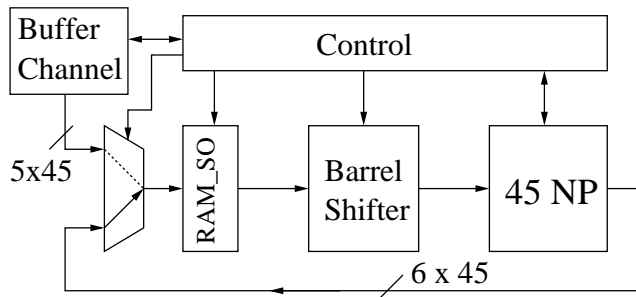


Fig. 11 Layered decoder architecture

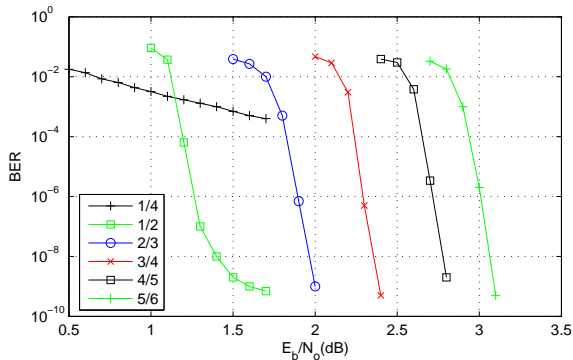


Fig. 12 BER for long frames

duce the buffer size. Note that the saturation and quantization solutions described in Section 3 for memory area saving also leads to area reductions of the NP and the barrel shifter. The latency in the CN core is also reduced due to the complexity reduction of the addition and comparison hardware.

6 Results

6.1 Performance results

Fig. 12 shows simulation results for code rates 1/4, 1/2, 2/3, 3/4, 4/5 and 5/6 with the 5-6-5 configuration. The code rates 2/3, 3/4, 4/5 and 5/6 fulfill the standard requirements. The code rate 1/4 shows poor performance. The code rates 1/4, 1/3 and 2/5 have a CN degree smaller than 7 (4, 5 and 6 respectively), which leads to an error floor when using the normalized Min-Sum algorithm. Note that code rate of 1/2, with a CN degree of 7, produces an error floor that can be corrected with the BCH outer decoder. The error floor produced by low code rates can be solved by implementing an A-min* or λ -min algorithm instead of the normalized Min-Sum in the NP, with no change in the rest of the architecture. It is also possible to implement a Sum-Product algorithm, described in [17], combined with the proposed saturation processes.

XQ5VLX85	LUT	LUT RAM	BRAM
Node Processor	143	2	0
sorting	37	0	0
gen $m_{c \rightarrow v}$	34	0	0
fifo $m_{v \rightarrow c}$	12	2	0
$m_{c \rightarrow v}$ memory	46	0	3
Total 1 node	189	2	3
Total 45 nodes	8586	90	135
Control	667	3	0
block SO RAM	360	0	22
Channel RAM	48	0	25
Barrel shifter	945	0	0
Total	11005	93	182
Percentage [%]	5	1	50

Table 3 Synthesis Results for DVB-S2 LDPC decoder

Paper	[20]	[29]	[30]	This
Parallelism	180	360	180	45
Air Throughput [Mb/s]	180	135	135	120
Extrinsic [bits]	6	6	6	5
SO_{ram} [bits]	10	8	8	6
Channel [bits]	6	6	6	5
Capacity [Mbits]	2.61	2.83	3.18	2.0

Table 4 Memory capacity comparison

6.2 Implementation results

The architecture presented in Fig. 11 was synthesized on a Virtex-V Pro FPGA (XQ5VLX110) from Xilinx for validation purposes. The system decodes long frames of code rate 2/3 and a parallelism of 45. Table 3 gives the hardware resources required. The clock frequency is 200 Mhz, the average number of iterations is 20 and the maximum average air throughput is 120 Mbps, which allows for the decoding of two simultaneous High-Definition Television (HDTV) streams.

The state-of-the-art provides results for different technologies, architectures and sub-optimal algorithm implementations which make comparison difficult. However, the number of NPs and the required memory capacity are fair points of comparison to highlight our contributions.

The implementation of a layered decoder for the DVB-S2 standard was considered in [20], [29] and [30]. Table 4 considers these implementations for comparison in terms of parallelism, air throughput and signal width. The parallelism provides information on the number of implemented NPs and an indication on the shuffling network complexity. The air throughput is in all cases higher than the standard requirement defined at 90 Mbps. The extrinsic and SO_{ram} word width directly impact on the memory size and the NP complexity. the number of bits for the main memory units. Note

that no information is provided on the ROM memories that store the matrices for every rate. In our architecture, a buffer of size two is added to store the channel LLR values to halve the average number of iteration as described in [28].

Thanks to the proposed saturation solution, our architecture provides significant memory savings independently of the considered suboptimal algorithm.

7 Conclusion

In this paper, we have presented optimization solutions for a layered LDPC decoder. Our first approach was to analyze the saturation problem in the layered decoder. An efficient saturation leads mainly to a reduction of memory area and also a reduction of latency in the computing elements. We developed a finite precision layered decoder architecture that implements the proposed saturation solution. This architecture outperforms the state-of-the-art in terms of memory needs while satisfying the standard requirements in terms of performance. In our second approach, we studied the problem of implementing an efficient multi-code-rate decoder. Our solution relied on the word split of the extrinsic memory for the Min-Sum algorithm. This solution allows for the use of single port RAMs and leads to significant memory reduction. Even though we have only considered the DVB-S2 standard in our study, the proposed techniques can be extended to DVB-T2, C2 and to any layered LDPC decoder. Future work will be dedicated to optimizing the hardware implementation (area and frequency) of the proposed decoder architecture and to the evaluation of its performance at low BER.

References

1. R. Gallager, *Low-Density Parity-Check Codes*. PhD thesis, Cambridge, 1963.
2. D. MacKay, "Good error-correcting codes based on very sparse matrices," *Information Theory, IEEE Transactions on*, vol. 45, pp. 399–431, Mar. 1999.
3. M. M. Mansour and N. R. Shanbhag, "High-throughput LDPC decoders," *IEEE Transactions on Very Large Scale Integration VLSI Systems*, vol. 11, pp. 976–996, Dec. 2003.
4. T. Brack, M. Alles, F. Kienle, and N. Wehn, "A synthesizable IP core for WIMAX 802.16e LDPC code decoding," in *Personal, Indoor and Mobile Radio Communications, 2006 IEEE 17th International Symposium on*, (Helsinki, Finland), pp. 1–5, Sept. 2006.
5. M. Rovini, F. Rossi, P. Ciao, N. L'Insalata, and L. Fanucci, "Layered decoding of non-layered LDPC codes," in *Digital System Design: Architectures, Methods and Tools, 2006. DSD 2006. 9th EUROMICRO Conference on*, (Dubrovnik, Croatia), pp. 537–544, Sept. 2006.
6. D. Hocevar, "A reduced complexity decoder architecture via layered decoding of LDPC codes," in *Signal Processing Systems, 2004. SIPS 2004. IEEE Workshop on*, (Austin, USA), pp. 107–112, Oct. 2004.
7. M. Fossorier, M. Mihaljevic, and H. Imai, "Reduced complexity iterative decoding of low-density parity check codes based on belief propagation," *IEEE Transactions on communications*, vol. 47, pp. 673–680, May 1999.
8. R. Tanner, "A recursive approach to low complexity codes," *Information Theory, IEEE Transactions on*, vol. 27, pp. 533–547, Sept. 1981.
9. D. MacKay and R. Neal, "Near Shannon limit performance of low density parity check codes," *Electronics Letters*, vol. 33, pp. 457–458, Mar. 1997.
10. M. Mansour and N. Shanbhag, "Low-power VLSI decoder architectures for LDPC codes," in *Low Power Electronics and Design, 2002. ISLPED '02. Proceedings of the 2002 International Symposium on*, (Monterey, USA), pp. 284–289, Aug. 2002.
11. I. std, "Air interface for fixed and mobile broadband wireless access systems," in *P802.16e/D12 Draft*, (Washington, DC, USA), pp. 100–105, IEEE, 2005.
12. Y. Sun, M. Karkooti, and J. Cavallaro, "High throughput, parallel, scalable LDPC encoder/decoder architecture for OFDM systems," in *Design, Applications, Integration and Software, 2006 IEEE Dallas/CAS Workshop on*, (Richardson, USA), pp. 39–42, Oct. 2006.
13. J. Dielissen, A. Hekstra, and V. Berg, "Low cost LDPC decoder for DVB-S2," in *Design, Automation and Test in Europe, 2006. DATE '06. Proceedings*, vol. 2, (Munich, Germany), pp. 1–6, Mar. 2006.
14. A. Segard, F. Verdier, D. Declercq, and P. Urard, "A DVB-S2 compliant LDPC decoder integrating the horizontal shuffle schedule," in *IEEE International Symposium on Intelligent Signal Processing and Communication Systems (ISPACS 2006)*, (Tottori, Japan), Dec. 2006.
15. T. Bhatt, V. Sundaramurthy, V. Stolpman, and D. McCain, "Pipelined block-serial decoder architecture for structured LDPC codes," in *Acoustics, Speech and Signal Processing, 2006. ICASSP 2006 Proceedings. 2006 IEEE International Conference on*, vol. 4, (Toulouse, France), p. IV, May 2006.
16. M. Rovini, G. Gentile, F. Rossi, and L. Fanucci, "A minimum-latency block-serial architecture of a decoder for IEEE 802.11n LDPC codes," in *Very Large Scale Integration, 2007. VLSI - SoC 2007. IFIP International Conference on*, (Atlanta, USA), pp. 236–241, Oct. 2007.
17. X.-Y. Hu, E. Eleftheriou, D.-M. Arnold, and A. Dholakia, "Efficient implementations of the sum-product algorithm for decoding LDPC codes," in *Global Telecommunications Conference, 2001. GLOBECOM '01. IEEE*, vol. 2, pp. 1036–1036E vol.2, 2001.
18. C. Jones, E. Valles, M. Smith, and J. Villasenor, "Approximate-min* constraint node updating for LDPC code decoding," in *IEEE Military Communication Conference*, pp. 157–162, Oct. 2003.
19. F. Guilloud, E. Boutillon, and J.-L. Danger, "lambda-min decoding algorithm of regular and irregular LDPC codes," *Proceedings of the 3rd International Symposium on Turbo Codes and Related Topics*, Sept. 2003.
20. S. Muller, M. Schreger, M. Kabutz, M. Alles, F. Kienle, and N. Wehn, "A novel LDPC decoder for DVB-S2 IP," in *Design, Automation & Test in Europe Conference & Exhibition, 2009. Date '09.*, (Nice, France), Apr. 2009.
21. J. Doré, *Optimisation conjointe des codes LDPC et de leurs architecture de décodage et mise en oeuvre sur FPGA*. PhD thesis, INSA, Rennes, France, 2007.

22. S. Papaharalabos and P. Mathiopoulos, "Simplified sum-product algorithm for decoding LDPC codes with optimale performance," *Electronics letters*, vol. 45, pp. 536–539, June 2009.
23. M. Gones, G. Falcao, J. Goncalves, V. Silva, M. Falcao, and P. Faia, "HDL library of processing units for generic and DVB-S2 LDPC decoding," in *International Conference on Signal Processing and Multimedia Applications (SIGMAP2006)*, (Setubal, Portugal), 2006.
24. O. Eljamaly and P. Sweeney, "Alternative approximation of check node algorithm for DVB-S2 LDPC decoder," in *Second International Conference on Systems and Networks Communications (ICSNC 2007)*, pp. 157–162, Oct. 2007.
25. A. Andreev, A. Bolotov, and R. Scepanovic, "Fifo memory with single port memory modules for allowing simultaneous read and write operations," *US patent 7181563*, Feb. 2007.
26. C. Marchand, J.-B. Doré, L. Conde-Canencia, and E. Boutillon, "Conflict resolution for pipelined layered LDPC decoders," in *Signal Processing Systems, 2009. SiPS 2009. IEEE Workshop on*, (Tampere, Finlande), pp. 220–225, Nov. 2009.
27. C. Marchand, J.-B. Doré, L. Conde-Canencia, and E. Boutillon, "Conflict resolution by matrix reordering for DVB-T2 LDPC decoders," in *Global Telecommunications Conference, 2009. GLOBECOM 2009. IEEE*, (Honolulu, USA), pp. 1–6, Nov. 2009.
28. M. Rovini and A. Martinez, "On the addition of an input buffer to an iterative decoder for LDPC codes," in *IEEE 65th Vehicular Technology Conference, VTC2007*, (Dublin, Ireland), pp. 1995–1999, Apr. 2007.
29. P. Urard, E. Yeo, L. Paumier, P. Georgelin, T. Michel, V. Lebars, E. Lantreibecq, and B. Gupta, "A 135mb/s DVB-S2 compliant codec based on 64800b LDPC and BCH codes," in *Solid-State Circuit Conference, 2005. Digest of Technical Papers. ISSCC. 2005 IEEE International*, (San Francisco, USA), pp. 446–447, Feb. 2005.
30. P. Urard, L. Paumier, V. Heinrich, N. Raina, and N. Chawla, "A 360mw 105b/s DVB-S2 compliant codec based on 64800b LDPC and BCH codes enabling satellite- transmission portble devices," in *Solid-State Circuits Conference, 2008. ISSCC 2008. Digest of Technical Papers. IEEE International*, (San Francisco, USA), pp. 310–311, Feb. 2008.



Cédric Marchand was born in 1976, France. He received the B.E. degree in electrical and electronics engineering from the North East Wales Institute, Wrexhan, Wales, 1999, M.Sc. and Ph.D. degrees in electrical engineering from the Université Européenne de Bretagne in 2007 and 2011 respectively. From 2007 to 2011, he has been working with NXP Semiconductor France on the implementation of an LDPC decoder for the DVB-S2, -

T2 and -C2 standards. His current research interests include error correcting code decoder and VLSI design.



Laura Conde-Canencia received her M.Sc. degree from Universidad Politecnica de Madrid, Spain, in 2000,

and Ph.D. from Telecom Bretagne, Brest, France, in 2004. Her Ph.D. thesis dealt with spectral-efficiency maximization in high-performance digital communication systems. In 2004, she joined Universidad San Pablo-CEU, in Madrid (Spain), as an Assistant Professor in Telecommunication Engineering. In 2006, she joined the LabSTICC Laboratory in Université de Bretagne Sud (Brittany, France), where she is currently an Associate Professor. Her research interests include Advanced Channel Coding such as Turbo-Codes, LDPC Codes and Cortex codes, focussing on decoder designs.



Emmanuel Boutillon was born in 1966, France. He received the Engineering Diploma from the Ecole Nationale Supérieure des Telecommunications (ENST), Paris, France in 1990. In 1991, he worked as assistant professor in the Ecole Multinationale Supérieure des Télécommunications in Dakar (Senegal). In 1992, he joined ENST as research engineer where he

had conducted research in the field of VLSI for digital communications. While he was working as engineer, he obtained his Ph.D in 1995 from ENST. In 1998, he spent a sabbatical year at the University of Toronto, Ontario, Canada. In 2000, he joined the Lab-STICC laboratory (Université de Bretagne Sud, Lorient, France) as Professor. His current research interests deal with the interactions between algorithm and architecture in the field of wireless communications. In particular, he works on Turbo Codes and LDPC decoders.